

Engineering the Substitution Position of Diphenylphosphine Oxide at Carbazole for Thermal Stability and High External Quantum Efficiency Above 30% in Blue Phosphorescent Organic Light-Emitting Diodes

Mounggon Kim and Jun Yeob Lee*

A carbazole derivative substituted with two diphenylphosphine oxide groups at asymmetric positions of carbazole is synthesized and the substitution position is correlated with the photophysical properties and device performances of blue phosphorescent organic light-emitting diodes. The carbazole type host with substituents at 2- and 5- positions of carbazole shows the merits of low driving voltage of 2-position substitution, and high thermal stability and high quantum efficiency of 5- position substitution. Therefore, the carbazole type host exhibits excellent thermal and morphological stability up to 140 °C and record high quantum efficiency of 31.4% and power efficiency of 53.1 lm W⁻¹ without any outcoupling enhancement and p- or n-doped charge transport layer in blue phosphorescent organic light-emitting diodes.

materials with bipolar charge transport properties.^[6–11] Another method was to substitute the electron transport unit at 2- or 3- positions of carbazole.^[12–14] The substitution enhanced the electron transport properties of carbazole derivatives, resulting in high quantum efficiency. The other method was to attach electron transport units at 2,7- or 3,6- positions of carbazole.^[12,15–19] Two electron transport units were symmetrically attached to the carbazole unit for better electron transport properties. Diphenylphosphine oxide, fluorene and imidazole moieties were attached to the carbazole core and balanced holes and electrons in the emitting layer.

1. Introduction

External quantum efficiency is one of the most important device characteristics of phosphorescent organic light-emitting diodes (PHOLEDs) because PHOLEDs can achieve 100% internal quantum efficiency, much higher than conventional fluorescent organic light-emitting diodes.^[1] The maximum external quantum efficiency of PHOLEDs was improved above 20% in red, green and blue PHOLEDs compared with 10% of that of fluorescent organic light-emitting diodes.^[2–4]

The advance of the quantum efficiency of PHOLEDs was made through development of triplet host materials. Typically, carbazole based host materials were effective to improve the quantum efficiency of PHOLEDs.^[4–11] The carbazole unit was typically used as a hole transport unit of host materials due to electron donating character of amine unit of carbazole and it was modified with electron transport units in various ways. Substitution of amine unit of carbazole was one of the most widely used methods to improve the electron transport properties of carbazole. Several carbazole derivatives with a substituent at nitrogen of carbazole were reported as the triplet host

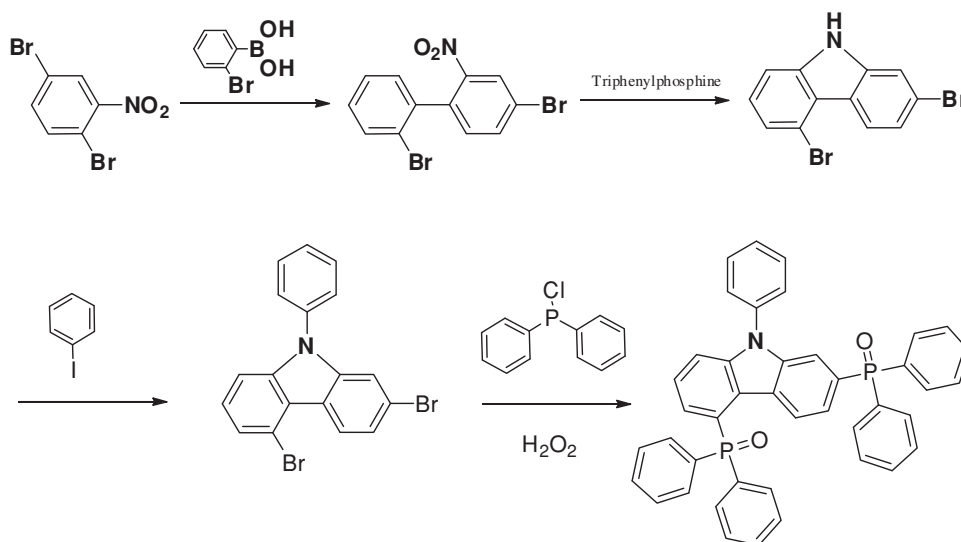
In general, the symmetric substitution of the carbazole core was made through bromination of carbazole^[12,18,19] or ring closing reaction of biphenyl with nitro functional group at *ortho*- position.^[17] However, it was difficult to brominate the carbazole unit asymmetrically because typical bromination of the carbazole unit results in symmetric bromination of the carbazole core. Asymmetric bromination may produce a carbazole derivative with the same functional units asymmetrically. The asymmetric substitution can improve the morphological stability of the host film due to suppressed molecular packing and manage the device performances of the host materials. Therefore, it is strongly required to develop carbazole derivatives with substituents at asymmetric position of carbazole.

Herein, we describe the synthesis of a carbazole derivative with electron withdrawing units at asymmetric positions of carbazole, (9-phenyl-9H-carbazole-2,5-diyl)bis(diphenylphosphine oxide) (PCPO25) and device performances of blue PHOLEDs with the carbazole derivative as the host material. It was demonstrated that the substitution of diphenylphosphine oxide at asymmetric positions of carbazole improved the glass transition temperature and morphological stability of the host material, power efficiency and quantum efficiency of the blue PHOLEDs. A high external quantum efficiency of 31.4% was achieved using the PCPO25 host material and the quantum efficiency obtained in this work is the best quantum efficiency value reported for blue PHOLEDs.^[6] It was even better than the state of the art quantum efficiency of red and green PHOLEDs.^[2,20]

M. Kim, Prof. J. Y. Lee
Department of Polymer Science and Engineering
Dankook University 126, Jukjeon-dong
Suji-gu, Yongin, Gyeonggi 448-701, Korea
E-mail: leej17@dankook.ac.kr



DOI: 10.1002/adfm.201304072



Scheme 1. Synthetic scheme of PCPO25.

2. Results and Discussion

The PCPO25 host material was designed to take advantage of the merits of good charge transport properties and low bandgap of substitution at 2- position of carbazole, and high glass transition temperature and high quantum efficiency of substitution at 4- position of carbazole.^[14] It was reported that substitution of diphenylphosphine oxide at 2- position of carbazole reduced the bandgap and increased charge transport properties because of deepened LUMO level, resulting in low driving voltage and high power efficiency in blue PHOLEDs.^[17] On the other hand, the substitution of diphenylphosphine oxide at 4- position of carbazole was effective to increase the glass transition temperature and quantum efficiency of blue PHOLEDs due to steric hindrance and balanced charge density.^[14] Therefore, the substitution of the diphenylphosphine oxide at 2- and 5- positions may have synergic effect on the thermal stability, low driving voltage and high quantum efficiency.

The PCPO25 host material was synthesized from a brominated carbazole intermediate with two bromine units at 2- and 5- positions of carbazole as shown in synthetic scheme in Scheme 1. The brominated intermediate was synthesized by ring closing reaction of 2',4'-bromo-2-nitro-1,1'-biphenyl which was synthesized by Suzuki coupling reaction between 1,4-dibromo-2-nitrobenzene and 2-bromophenylboronic acid. The synthetic yield of the PCPO25 compound was 62.4% from the brominated intermediate and the synthetic yield of the ring closing reaction was 88.7%. The PCPO25 host material was purified by vacuum train sublimation to obtain high purity level above 99% from high performance liquid chromatography analysis.

The photophysical properties of the PCPO25 were measured using ultraviolet-visible (UV-Vis) and photoluminescence (PL) spectrometers. Figure 1 shows UV-Vis and PL spectra of the PCPO25 host material. PCPO25 showed $n-\pi^*$ absorption of carbazole at 335, 355, and 371 nm, and $\pi-\pi^*$ absorption of diphenylphosphine oxide modified carbazole at 261, 304, and 313 nm. The UV-Vis absorption of carbazole was similar to

that of PPO27 with two diphenylphosphine oxide units symmetrically.^[17] The absorption edge of the UV-Vis absorption was 379 nm (bandgap of 3.27 eV), which was similar to that of PPO27. This indicates that the substitution at 2- position of carbazole dominates the photophysical properties of PCPO25. Solution PL emission of PCPO25 was observed at 385 nm and 398 nm and solid PL emission was shifted to long wavelength due to intermolecular interaction in solid state. Phosphorescent emission of PCPO25 was analyzed at 77 K and first phosphorescent emission peak appeared at 443 nm. High triplet energy of 2.80 eV was calculated from the first phosphorescent emission peak, which was the same as that of PPO27 with substituents at symmetric position.^[17] All photophysical properties of PCPO25 were similar to those of PPO27 because of the diphenylphosphine oxide substitution at 2- position. The substitution at 5- position had little effect on the photophysical properties of PCPO25.

The highest occupied molecular orbital (HOMO) of PCPO25 was measured by cyclic voltammetry and the lowest unoccupied molecular orbital (LUMO) of PCPO25 were calculated from

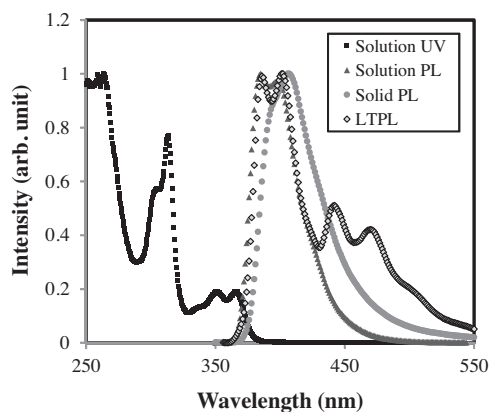


Figure 1. UV-Vis absorption, solution PL, solid PL and low temperature PL (LTPL) spectra of PCPO25.

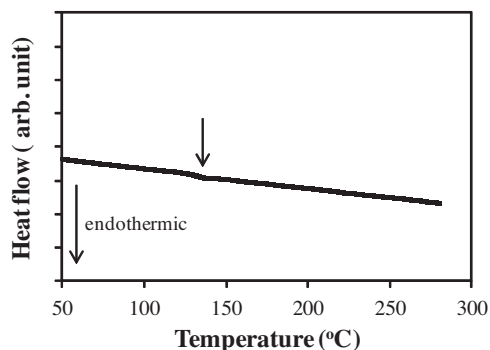


Figure 2. DSC thermogram of PCPO25.

the HOMO and bandgap from UV-Vis absorption edge. The HOMO and the LUMO of PCPO25 were -6.17 eV and -2.90 eV, respectively, which were suitable for hole injection from mCP hole transport layer (-6.10 eV) and electron injection from TSP01 electron transport layer (-2.52 eV).

Thermal stability of PCPO25 was studied using differential scanning calorimeter (DSC) and thermogravimetric analyzer (TGA). DSC and TGA thermograms of PCPO25 are shown in Figure 2 and Figure 3. Glass transition temperature (T_g) was measured from the inflection point of DSC thermogram and it was 140 °C, which was higher than that of PPO27 (120 °C) and PPO36 (123 °C) with two diphenylphosphine oxide units at symmetrical positions.^[17] The high T_g of PCPO25 can be explained by the substitution of diphenylphosphine oxide at 5-position, which induces steric hindrance and restricted molecular motion. The rotation of the diphenylphosphine oxide unit is hindered by the carbazole core, resulting in high T_g . The substitution of diphenylphosphine oxide at 5-position increased the T_g although it did not affect the photophysical properties of PCPO25. The improved thermal stability was also confirmed by TGA and the thermal decomposition temperature at 5% weight loss was 506 °C, which was much higher than that of PPO27 with substituents at symmetric positions.

The thermal stability of the PCPO25 was also confirmed by monitoring the crystallization and PL emission of PCPO25: iridium(III) bis[(4,6-difluorophenyl)-pyridinato- N,C^2]picolinate (FIrpic) film deposited by vacuum thermal evaporation at high temperature. The PCPO25:FIrpic film was annealed from 100 °C to check the film stability. Optical microscopic pictures of PCPO25:FIrpic films are presented in Figure 4 according

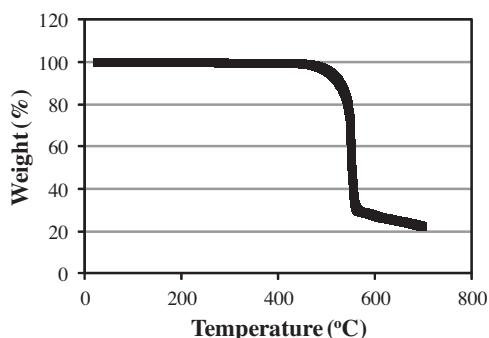


Figure 3. TGA thermogram of PCPO25.

to annealing temperature after 10 min annealing at the annealing temperature. There was no crystallization observed up to 150 °C, which proves the excellent thermal stability of the PCPO25 film. PL intensity of the PCPO25:FIrpic film was also not greatly affected by the high temperature annealing up to 130 °C as shown in Figure S1 in Supporting Information. Above 95% of the original PL emission was maintained up to 130 °C. The high T_g and morphological stability of the PCPO25 contributed to the stable PL intensity after thermal treatment at high temperature.

Hole only and electron only devices of PCPO25 were fabricated to compare hole and electron densities in the PCPO25 device. Figure 5 shows current density-voltage curves of hole and electron only devices of PCPO25. Device structures of hole only and electron only devices were indium tin oxide (ITO, 50 nm)/poly(3,4-ethylenedioxythiophene) : poly(styrenesulfonate) (PEDOT:PSS, 60 nm)/4,4'-cyclohexylidenebis[N,N-bis(4-methylphenyl)aniline] (TAPC, 20 nm)/1,3-bis(N-carbazolyl)benzene (mCP, 10 nm)/PCPO25 (25 nm)/TAPC (5 nm)/Al (200 nm) and ITO (50 nm)/Ca (5 nm)/PCPO25 (25 nm)/diphenylphosphine oxide-4-(triphenylsilyl)phenyl (TSP01, 35 nm)/LiF (1 nm)/Al (200 nm), respectively. The hole and electron current densities of the PCPO25 host were similar over all voltage ranges measured, which indicates that holes and electrons can be balanced in the emitting layer. As there was little energy barrier for hole and electron injection, the similar hole and electron current density of the single carrier devices reflects bipolar charge transport properties of the PCPO25 host. As reported in other works, the combination of electron donating carbazole and electron withdrawing diphenylphosphine oxide units induced the similar hole and electron current densities in the single charge devices.^[12]

The PCPO25 host was evaluated as the host material for blue PHOLEDs because PCPO25 possessed high triplet energy of 2.80 eV for efficient energy transfer to FIrpic dopant material. Figure 6 shows current density-voltage-luminance curves of the blue PHOLEDs with the PCPO25 host material according to the doping concentration of FIrpic. The doping concentrations of FIrpic were 5, 10, and 20%. The current density of the blue PHOLEDs was increased according to the increase of FIrpic doping concentration. As reported in other works, the better charge hopping between dopant materials enhanced the current density at high doping concentration.^[21] However, the luminance showed a maximum value at 10% doping concentration due to poor recombination efficiency and concentration quenching effect at 20% doping concentration, which will be shown in Figure 7. Turn-on voltage of the device was 3.0 V and the driving voltage at 1000 cd m $^{-2}$ was 5.1 V, which was similar to that of PPO27 based blue device. Although the diphenylphosphine oxide was substituted at 2- and 5- positions, the driving voltage could be lowered just as the PPO27 host with two substituents at 2- and 7- positions.

Quantum efficiency-luminance curves of the PCPO25 blue PHOLEDs are shown in Figure 7. The quantum efficiency of the PCPO25 blue PHOLEDs was optimized at 10% doping concentration and a maximum quantum efficiency of 31.4% was achieved at 100 cd m $^{-2}$ without any out-coupling enhancement. The high quantum efficiency was maintained even at high luminance and a quantum efficiency of 28.6% was obtained at



Figure 4. Optical microscopic pictures of PCPO25 according to annealing temperature after 10 min annealing at the test temperature.

1000 cd m^{-2} . The external quantum efficiency of the PCPO25 device is better than any other data reported in blue devices.^[6] The high quantum efficiency of the PCPO25 blue PHOLEDs can be explained by efficient energy transfer (high PL intensity), charge balance and exciton confinement. Energy transfer from PCPO25 to FIrpic is critical to the quantum efficiency, which was confirmed by PL emission of PCPO25:FIrpic film compared with that of mCP:FIrpic film (Figure S2 in Supporting Information). The PL emission intensity of the PCPO25:FIrpic film was stronger than that of mCP:FIrpic film, which confirms the efficient energy transfer from PCPO25 to FIrpic. Absolute PL quantum efficiency of PCPO25:FIrpic film was $95 \pm 5\%$ from integrating sphere measurement, which confirms the efficient energy transfer from PCPO25 to FIrpic. In addition, the PL emission was not reduced up to 10% doping concentration, indicating that the PCPO25 host suppressed triplet-triplet annihilation at high doping concentration.

Holes and electrons balance in the emitting layer also contributed to the above 30% quantum efficiency of the PCPO25 devices. As shown in the single charge device data, PCPO25 showed similar hole and electron current density, which balanced holes and electrons in the emitting layer, enhancing the quantum efficiency. The exciton confinement is also a key factor for the high quantum efficiency of the PCPO25 blue devices. Triplet excitons of FIrpic are effectively confined inside the PCPO25 emitting layer because of high triplet energy of mCP (2.90 eV) and TSPO1 (3.39 eV) charge transport materials. The triplet excitons of FIrpic are not quenched by PCPO25, mCP and TSPO1 which are in direct contact with FIrpic, which improved the external quantum efficiency of PCPO25

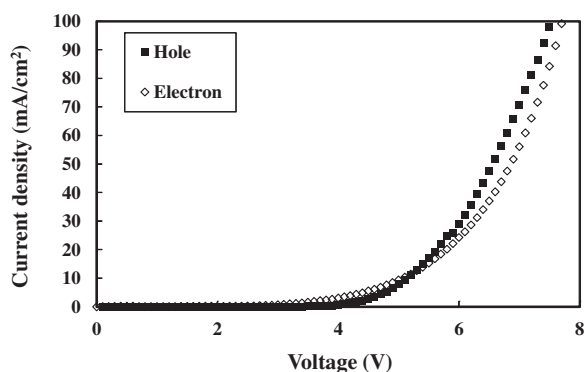


Figure 5. Current density-voltage curves of hole only and electron only devices of PCPO25.

devices. In addition, Lambertian distribution of light emission was confirmed and no out-coupling enhancement was observed in the PCPO25 device. In addition, the use of thin ITO electrode (50 nm) had positive effect on the quantum efficiency because of high transmittance in blue emitting wavelength region and suppressed waveguide mode.^[22] The quantum efficiency of the PCPO25 device was higher than that of PPO27 device (27.5%) and mCP device (19.7%).

The power efficiency of the PCPO25 blue PHOLEDs was also plotted against luminance. The maximum power efficiency of the PCPO25 blue device was 53.1 lm W^{-1} and the power efficiencies at 100 cd m^{-2} and 1000 cd m^{-2} were 46.9 lm W^{-1} and 33.5 lm W^{-1} , respectively. Although p- or n-doped charge transport layers were not used in this work, high power efficiency was obtained due to low driving voltage by substitution at 2- position and high quantum efficiency by substitution at 5- position.

Electroluminescence (EL) spectra of the PCPO25 blue PHOLEDs are shown in Figure 8. Although bathochromic shift of the EL spectra by 3 nm was observed at high doping concentration, only FIrpic emission peak was observed without any emission from the PCPO25 host. This confirms the efficient energy transfer from PCPO25 to FIrpic and charge confinement inside the emitting layer.

3. Conclusions

In conclusion, substitution of electron withdrawing groups at asymmetric position of carbazole was effective to improve the thermal stability and device performances of blue PHOLEDs simultaneously. The PCPO25 host with substituents at 2- and 5- positions showed the merits of low driving voltage of 2- position substitution and high thermal stability and high quantum efficiency of 5- position substitution. Therefore, the PCPO25 host exhibited excellent thermal and morphological stability up to 140 °C and record high quantum efficiency of 31.4% and power efficiency of 53.1 lm W^{-1} without any outcoupling enhancement and p- or n-doped charge transport layer in blue PHOLEDs. The quantum efficiency and power efficiency

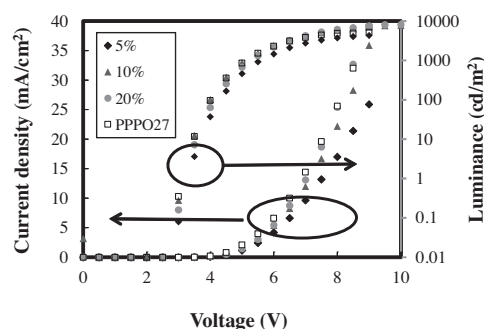


Figure 6. Current density-voltage-luminance curves of the PCPO25 devices according to the doping concentration of FIrpic. Device data of the PPO27 device were added for comparison.

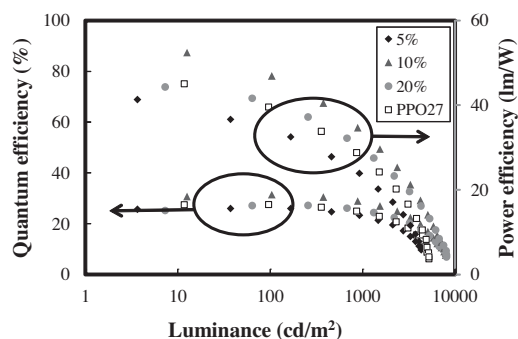


Figure 7. Quantum efficiency–power efficiency–luminance curves of the PCPO25 devices according to the doping concentration of Flrpic. Device data of the PPO27 device were added for comparison.

obtained in this work are the best efficiency values reported in blue PHOLEDs. Therefore, the modification of carbazole at asymmetric positions can be effective to improve the device performances of blue PHOLED in future development of host and charge transport materials.

4. Experimental Section

Synthesis of 2',4-Dibromo-2-nitro-1,1'-biphenyl: 1,4-Dibromo-2-nitrobenzene (3.0 g, 10.680 mmol), 2-bromophenylboronic acid (2.36 g, 11.748 mmol), and tetrakis(triphenylphosphine)palladium(0) (0.62 g, 0.534 mmol) were dissolved in tetrahydrofuran (60 mL) and aqueous K_2CO_3 (8.29 g, 2 M) solution (30 mL) was added. The solution was refluxed for 18 h and was extracted with methylene chloride and water after cooling to room temperature. The combined organic layer was dried over $MgSO_4$ and concentrated. Purification by silicagel chromatography using methylene chloride : n-hexane (1:9) gave a yellowish powder. The product was obtained to 2.6 g (yield 68.0%). 1H NMR (200 MHz, $CDCl_3$): δ 8.25 (s, 1H), 7.81 (d, 1H, $J = 8.0$ Hz), 7.65 (d, 1H, $J = 8.0$ Hz) 7.43–7.22 (m, 4H). MS (FAB) m/z 358[(M+H) $^+$].

Synthesis of 2,5-Dibromo-9H-carbazole: 2',4-Dibromo-2-nitro-1,1'-biphenyl (2.6 g, 7.283 mmol) and triphenylphosphine (4.78 g, 18.207 mmol) were dissolved in 1,2-dichlorobenzene (60 mL). The mixture was refluxed for 12 h and was extracted with methylene chloride and water after cooling to room temperature. The combined organic layer was dried over $MgSO_4$ and concentrated. Purification by silicagel chromatography using methylene chloride : n-hexane (1:9) gave a white powder. The product was obtained to 2.1 g (yield 88.7%). 1H NMR

(200 MHz, $CDCl_3$): δ 8.58 (d, 1H, $J = 8.0$ Hz), 7.60 (s, 1H, $J = 8.0$ Hz), 7.40–7.31 (m, 4H). MS (FAB) m/z 326[(M+H) $^+$].

Synthesis of 2,5-Dibromo-9-phenyl-9H-carbazole: 2,5-Dibromo-9H-carbazole (2.5 g, 7.692 mmol), iodobenzene (3.14 g, 15.385 mmol), copper iodide (0.73 g, 3.846 mmol) and K_2CO_3 (2.13 g, 15.385 mmol) were dissolved in 1,4-dioxane (60 mL) and ethylenediamine (0.42 mL, 3.846 mmol) was added to the solution. The mixture was refluxed for 24 h and was extracted using methylene chloride and water after cooling to room temperature. The combined organic layer was dried over $MgSO_4$ and concentrated. Purification by silicagel chromatography using n-hexane gave a white powder. The product was obtained to 2.6 g (yield 81.0%). 1H NMR (400 MHz, $CDCl_3$): δ 8.69 (d, 1H, $J = 16$ Hz), 7.63 (t, 1H, $J = 16.0$ Hz), 7.51–7.45 (m, 6H), 7.28–7.27 (m, 2H). MS (FAB) m/z 402[(M+H) $^+$].

Synthesis of (9-Phenyl-9H-carbazole-2,5-diyl)bis(diphenylphosphine oxide) (PCPO25): 2,5-Dibromo-9-phenyl-9H-carbazole (2.5 g, 6.233 mmol) was dissolved in tetrahydrofuran (40 mL) under argon at -78 °C followed by slow addition of n-butyllithium (8.96 mL, 1.6 M). Dichlorodiphenylphosphine (2.65 mL, 15.583 mmol) was added slowly to the solution after 1 h. The mixture was stirred for 2 h at -78 °C, and allowed to warm to room temperature. After overnight stirring, methanol (10 mL) was added to the solution for 2 h and the solution was extracted with water and methylene chloride. The combined organic layer was dried over $MgSO_4$ and concentrated. Purification by silicagel chromatography using methylene chloride : n-hexane (1:4) gave a white powder. After vacuum drying, the white powder was dissolved in a mixed solvent of methylene chloride and H_2O_2 (10:2 mL) and the solution was stirred for 2 h. After extraction with water and methylene chloride, the combined organic layer was dried over $MgSO_4$ and concentrated. The product was obtained to 2.5 g (yield 62.4%). 1H NMR (500 MHz, $CDCl_3$): δ 8.82 (d, 1H, $J = 10.0$ Hz), 7.95 (d, 1H, $J = 10.0$ Hz), 7.74–7.70 (m, 4H), 7.62–7.53 (m, 10H), 7.50–7.44 (m, 9H), 7.41–7.33 (m, 5H), 7.16 (t, 1H, $J = 10.0$ Hz). ^{13}C NMR (125 MHz, $CDCl_3$): δ 142.6, 142.5, 141.2, 141.1, 133.4, 132.8, 132.5, 132.2, 132.1, 132.0, 131.7, 130.2, 129.9, 129.2, 128.6, 128.5, 128.4, 128.3, 127.7, 127.1, 126.8, 126.3, 125.9, 125.8, 125.7, 125.6, 124.4, 123.2, 123.1, 114.5, 114.0. MS (FAB) m/z 644[(M+H) $^+$]. Anal. Calcd for $C_{42}H_{31}NO_2P_2$: C, 78.37; H, 4.85; N, 2.18; O, 4.97; P, 9.62. Found: C, 77.61; H, 4.86; N, 2.19.

Device Fabrication and Measurements: The device structure of blue PHOLEDs was ITO (50 nm)/PEDOT:PSS (60 nm)/TAPC (20 nm)/mCP (10 nm)/PCPO25:Flrpic (25 nm, x%)/TSPO1 (35 nm)/LiF (1 nm)/Al (200 nm). The doping concentrations of Flrpic were 5%, 10%, and 20%. Device structures of hole and electron devices were ITO (50 nm)/PEDOT:PSS (60 nm)/TAPC (20 nm)/mCP (10 nm)/PCPO25 (25 nm)/TAPC (5 nm)/Al and ITO (50 nm)/Ca (5 nm)/PCPO25 (25 nm)/TSPO1 (35 nm)/LiF (1 nm)/Al (200 nm), respectively. Vacuum thermal evaporation was used to fabricate the blue PHOLEDs and single carrier devices. Current density–voltage–luminance curves of blue PHOLEDs and single carrier devices were obtained using Keithley 2400 source measurement unit and CS1000 spectroradiometer.

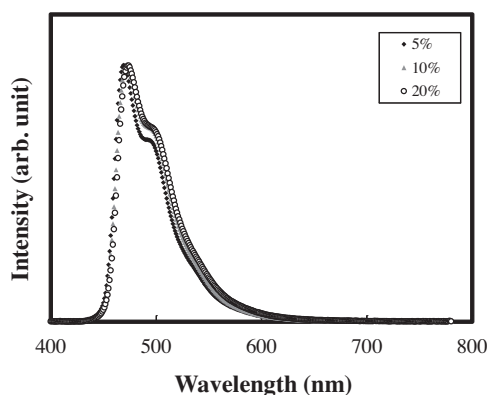


Figure 8. EL spectra of the PCPO25 devices according to the doping concentration of Flrpic.

Supporting Information

Supporting Information is available from the Wiley Online Library or from the author.

Received: December 4, 2013

Revised: February 13, 2014

Published online: March 28, 2014

- [1] M. A. Baldo, D. F. O'Brien, Y. You, A. Shoustikov, M. E. Thompson, S. R. Forrest, *Nature* **1998**, 395, 151.
- [2] S. Su, H. Sasabe, Y. Pu, K. Nakayama, J. Kido, *Adv. Mater.* **2010**, 22, 3311.
- [3] D. H. Kim, N. S. Cho, H. Oh, J. H. Yang, W. S. Jeon, J. S. Park, M. C. Suh, J. H. Kwon, *Adv. Mater.* **2011**, 23, 2721.

- [4] S. O. Jeon, S. E. Jang, H. S. Son, J. Y. Lee, *Adv. Mater.* **2011**, *23*, 1436.
- [5] L. Duan, J. Qiao, Y. Sun, Y. Qiu, *Adv. Mater.* **2011**, *23*, 1137.
- [6] J. Bin, N. Cho, J. Hong, *Adv. Mater.* **2012**, *24*, 2911.
- [7] H. Chou, C. Cheng, *Adv. Mater.* **2010**, *22*, 2468.
- [8] H. Sasabe, N. Toyota, H. Nakanishi, T. Ioshizaka, Y. Pu, J. Kido, *Adv. Mater.* **2012**, *24*, 3212.
- [9] C. W. Lee, J. Y. Lee, *Adv. Mater.* **2013**, *25*, 596.
- [10] Y. Tao, Q. Wang, C. Yang, Q. Wang, Z. Zhang, T. Zou, J. Qin, D. Ma, *Angew. Chem. Int. Ed.* **2008**, *47*, 8104.
- [11] L. S. Sapochak, A. B. Padmaperuma, X. Cai, J. L. Male, P. E. Burrows, *J. Phys. Chem. C* **2008**, *112*, 7989.
- [12] S. O. Jeon, K. S. Yook, C. W. Joo, J. Y. Lee, *Adv. Funct. Mater.* **2009**, *19*, 3644.
- [13] C. W. Lee, J. Y. Lee, *Chem. Commun.* **2013**, *49*, 1446.
- [14] M. Kim, J. Y. Lee, *Org. Electron.* **2013**, *14*, 67.
- [15] M.-H. Tsai, H.-W. Lin, H.-C. Su, T.-H. Ke, C. Wu, F.-C. Fang, Y.-L. Liao, K.-T. Wong, C.-I. Wu, *Adv. Mater.* **2006**, *18*, 1216.
- [16] P.-I. Shih, C.-H. Chien, C.-Y. Chuang, C.-F. Shu, C.-H. Yang, J.-H. Chen, Y. Chi, *J. Mater. Chem.* **2007**, *17*, 1692.
- [17] H. S. Son, C. W. Seo, J. Y. Lee, *J. Mater. Chem.* **2011**, *21*, 5638.
- [18] W. Hung, L. Chi, W. Chen, Y. Chen, S. Chou, K. Wong, *J. Mater. Chem.* **2010**, *20*, 10113.
- [19] J. Ding, Q. Wang, L. Zhao, D. Ma, L. Wang, X. Jing, F. Wang, *J. Mater. Chem.* **2010**, *20*, 8126.
- [20] S. Kim, W. Jeong, C. Mayr, Y. Park, K. Kim, J. Lee, C. Moon, W. Brutting, J. Kim, *Adv. Funct. Mater.* **2013**, *23*, 3896.
- [21] L. Hou, L. Duan, J. Qiao, W. Li, D. Zhang, Y. Qiu, *Appl. Phys. Lett.* **2008**, *92*, 263301.
- [22] H. H. Lu, J. R. Strum, *J. Appl. Phys.* **2002**, *91*, 595.